Cancer Cell
Article

Deletion of NEMO/IKKγ in Liver Parenchymal Cells Causes Steatohepatitis and Hepatocellular Carcinoma

Tom Luedde,[1,2] Naiara Beraza,[3] Vasileios Kotsikoris,[2] Geert van Loo,[2] Arianna Nenci,[2] Rita De Vos,[4] Tania Roskams,[4] Christian Trautwein,[3] and Manolis Pasparakis[1,2,*]
[1] Institute for Genetics, University of Cologne, Zülpicher Strasse 47, 50674 Cologne, Germany
[2] EMBL Mouse Biology Unit, via Ramarini 32, 00016 Monterotondo (Rome), Italy
[3] Medical Clinic III, University Hospital, RWTH Aachen, Pauwelsstrasse 30, 52074 Aachen, Germany
[4] Department of Pathology, University of Leuven, Minderbroederstraat 12, B-3000 Leuven, Belgium
*Correspondence: pasparakis@uni-koeln.de
DOI 10.1016/j.ccr.2006.12.016

SUMMARY

The IκB kinase (IKK) subunit NEMO/IKKγ is essential for activation of the transcription factor NF-κB, which regulates cellular responses to inflammation. The function of NEMO in the adult liver remains elusive. Here we show that ablation of NEMO in liver parenchymal cells caused the spontaneous development of hepatocellular carcinoma in mice. Tumor development was preceded by chronic liver disease resembling human nonalcoholic steatohepatitis (NASH). Antioxidant treatment and genetic ablation of FADD demonstrated that death receptor-mediated and oxidative stress-dependent death of NEMO-deficient hepatocytes triggered disease pathogenesis in this model. These results reveal that NEMO-mediated NF-κB activation in hepatocytes has an essential physiological function to prevent the spontaneous development of steatohepatitis and hepatocellular carcinoma, identifying NEMO as a tumor suppressor in the liver.

INTRODUCTION

The nuclear factor (NF)-κB signaling pathway mediates a variety of important cellular functions by regulating immune and inflammatory responses (Karin and Lin, 2002; Pahl, 1999). NF-κB transcription factors are kept inactive in the cytoplasm through binding to members of the IκB family of inhibitory proteins. Cell activation by a variety of stimuli induces the phosphorylation, polyubiquitination, and proteasome-dependent degradation of IκB proteins, allowing NF-κB dimers to accumulate in the nucleus (Karin and Lin, 2002; Pahl, 1999). The IκB kinase (IKK) complex, consisting of two catalytic subunits—IKK1/IKKα and IKK2/IKKβ—and a regulatory subunit called NF-κB-essential-modulator (NEMO/IKKγ), mediates NF-κB activation in response to a variety of stimuli by phosphorylating IκB proteins (Ghosh and Karin, 2002; Karin, 1999). Gene-targeting experiments showed that mice lacking p65/RelA, IKK2, or NEMO die during embryonic development due to liver apoptosis (Beg et al., 1995; Li et al., 1999a, 1999b; Tanaka et al., 1999; Rudolph et al., 2000; Schmidt-Supprian et al., 2000; Makris et al., 2000). Although these studies demonstrated the essential role of NF-κB in protecting the fetal liver from cell death, the physiological function of NF-κB in the adult liver remains elusive. Despite various attempts to address the function of NF-κB in the adult liver, previous studies failed to reveal a spontaneous phenotype caused by NF-κB inhibition in

SIGNIFICANCE

NF-κB is constitutively activated in many tumors and is thought to provide a critical survival signal that assists cancer cells to escape apoptosis. Thus, NF-κB inhibition is considered a promising approach in antitumor therapy. Our results presented here show that sensitization of hepatocytes to apoptosis by NF-κB inhibition causes steatohepatitis and hepatocellular carcinoma, providing a paradigm for the role of NF-κB in cancer. In addition, these findings suggest that NF-κB might provide a molecular link connecting inflammatory, survival, and metabolic pathways in the liver and may be relevant for the pathogenic mechanisms linking NASH to liver cancer in humans. These results highlight the need for extensive research on the potential side effects of drugs targeting the IKK/NF-κB pathway.

hepatocytes, either by conditional deletion of *Ikk2* or by transgenic overexpression of IκBα-super-repressors (Lavon et al., 2000; Chaisson et al., 2002; Maeda et al., 2003, 2005; Pikarsky et al., 2004; Luedde et al., 2005), suggesting that NF-κB is not essential for normal liver physiology.

Hepatocellular carcinoma is one of the most common cancers worldwide and develops frequently in the context of chronic hepatitis characterized by liver inflammation and hepatocyte apoptosis (Motola-Kuba et al., 2006; Okuda, 2000). However, the molecular mechanisms underlying this sequence of events are only poorly understood. Recently, the function of NF-κB signaling in the development of liver tumors has raised great interest. In one study, NF-κB inhibition by overexpression of a nondegradable IκBα super-repressor was shown to inhibit later stages of tumor progression in Mdr2-deficient mice, which develop hepatocellular carcinoma in the context of chronic bile duct inflammation (Pikarsky et al., 2004). On the other hand, deletion of *Ikk2* in hepatocytes resulted in increased tumor formation in a mouse model of chemical carcinogen-induced hepatocellular carcinomas (Maeda et al., 2005). These apparently contradicting conclusions may be influenced by differences in the inhibitory potential and the cell specificity of the methods used to block NF-κB, and also by the different tumor models applied. Therefore, the function of NF-κB in liver cancer seems to be complex, acting either as a tumor promoter or as a tumor suppressor.

Here we have investigated the function of the IKK subunit NEMO in liver physiology by generating mice with conditional ablation of NEMO in parenchymal liver cells. Ablation of NEMO but not IKK2 caused the spontaneous development of liver cancer, revealing a role of NEMO as a tumor suppressor in the liver. We show that tumor formation is preceded by the spontaneous development of chronic hepatitis resembling human nonalcoholic steatohepatitis (NASH). This process is initiated by the hypersensitivity of NEMO-deficient hepatocytes to spontaneous FADD-mediated and oxidative-stress-dependent death, which triggers compensatory hepatocyte proliferation, inflammation, and activation of liver progenitor cells. These results demonstrate that NEMO-dependent NF-κB activation has an essential physiological function to prevent spontaneous liver tumor development.

RESULTS

Spontaneous Development of Hepatocellular Carcinomas in NEMO$^{LPC\text{-}KO}$ Mice

Mice lacking NEMO die during embryonic development (Rudolph et al., 2000; Schmidt-Supprian et al., 2000; Makris et al., 2000). To investigate the role of NEMO and IKK2 in the adult liver, we generated mice with liver parenchymal cell-specific knockout of these subunits (NEMO$^{LPC\text{-}KO}$, IKK2$^{LPC\text{-}KO}$) by crossing mice carrying loxP-flanked *Nemo* (Schmidt-Supprian et al., 2000) or *Ikk2* (Pasparakis et al., 2002) alleles with *Alfp*-cre transgenics, which mediate efficient Cre recombination in liver parenchymal cells, including hepatocytes and biliary epithelial cells, but not in endothelial or Kupffer cells (Coffinier et al., 2002; Kellendonk et al., 2000). NEMO$^{LPC\text{-}KO}$ mice were born and reached weaning age at the expected Mendelian frequency. NEMO$^{LPC\text{-}KO}$ mice and IKK2$^{LPC\text{-}KO}$ mice showed efficient ablation of the respective proteins in whole-liver extracts (Figure 1A). Low residual expression of NEMO and IKK2 in these mice can be attributed to nonparenchymal liver cells that are not targeted by the Alfp-cre construct. Accordingly, primary hepatocytes isolated from NEMO$^{LPC\text{-}KO}$ and IKK2$^{LPC\text{-}KO}$ mice showed complete lack of NEMO and IKK2, respectively (Figure 1B).

Dissection of livers from 12-month-old male NEMO$^{LPC\text{-}KO}$ mice surprisingly revealed the presence of multiple large tumors (Figures 1C and 1D). No tumors were detected either in the liver of littermates carrying the NEMO loxP flanked allele but lacking Cre recombinase expression (Figure 1E), which were used as wild-type controls in all experiments described here, or in IKK2$^{LPC\text{-}KO}$ mice at the same age (Figure 1F). Histological analysis revealed the presence of malignant liver tumors corresponding to well- to moderately differentiated hepatocellular carcinomas (Figures 1I–1N), as well as premalignant liver tumors (dysplastic foci, low-grade and high-grade dysplastic nodules; Figure 1H). Malignant liver tumors, as defined histologically by the International Working Party (1995) (Kojiro and Roskams, 2005), were detected in all 14 male mice examined at this age. The average number of malignant liver tumors per mouse was 5.75 (standard deviation [SD] = 3.09) with an average size of 8.58 mm (SD = 3.01 mm). Malignant liver tumors were characterized by expansive growth (Figures 1I–1K), increased cellularity, a broad trabecular growth pattern in four to six layers, increased eosinophilia, a higher nuclear to cytoplasmic index compared to hepatocytes in nontumor areas (compare Figure 1L [HCC] to Figure 1M [nonmalignant]), and complete absence of portal tracts even within large tumor areas (Figures 1I–1K). Moreover, malignant liver tumors displayed a strongly increased proliferation as shown by increased BrdU incorporation (Figure S1 in the Supplemental Data available with this article online) and by counting mitotic figures (average of 1.44 mitotic figures per high-power field [hpf] with a range between 1.13 and 2.79 mitotic figures per hpf in different tumors, compared to 0.13 mitotic figures per hpf in nonmalignant areas) (Figure 1N). In livers from NEMO$^{LPC\text{-}KO}$ mice at 9 months of age, dysplastic foci and nodules but no malignant tumors were found (data not shown), suggesting that malignant tumors arise between 9 and 12 months of age. To verify deletion of NEMO in malignant liver tumors in NEMO$^{LPC\text{-}KO}$ mice, we performed immunoblot and immunofluorescence analyses on dissected tumor tissue and found that tumors lack NEMO expression (Figure S2). Taken together, these results demonstrate that conditional deletion of *Nemo* but not *Ikk2* in parenchymal liver cells results in spontaneous development of hepatocellular carcinomas in mice, revealing a function of NEMO as a tumor suppressor in the liver.

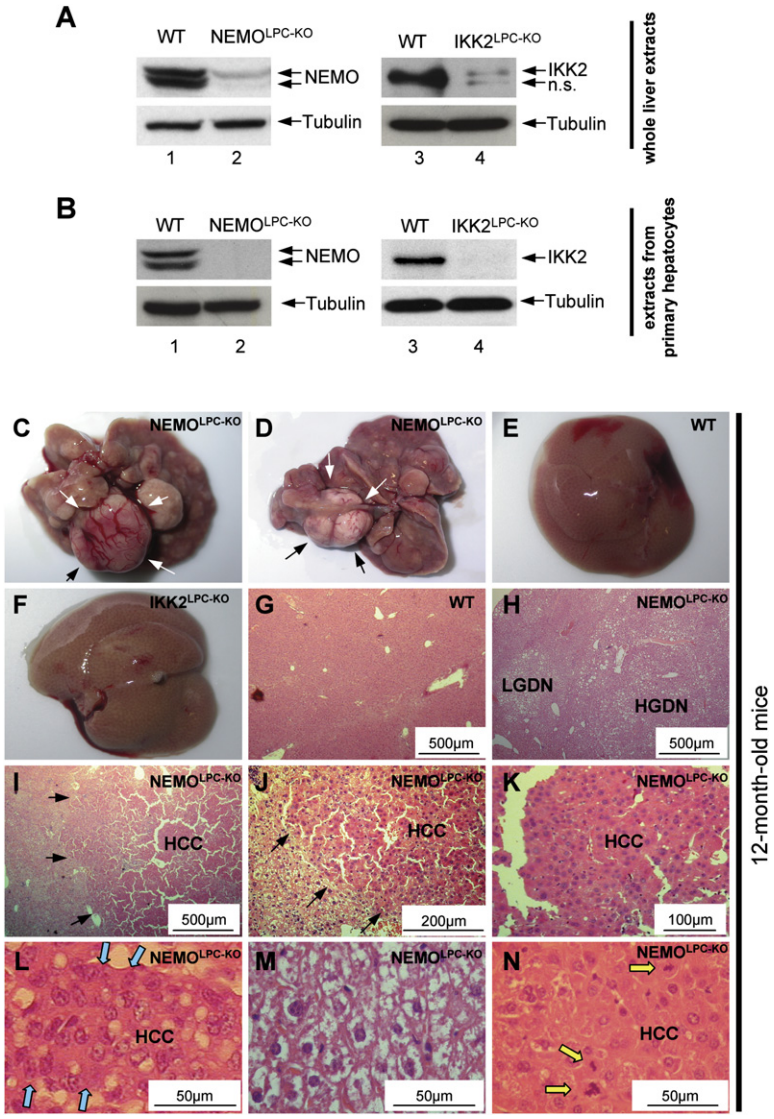

Figure 1. Spontaneous Development of Liver Tumors in NEMO^{LPC-KO} Mice

(A) Liver extracts from 8-week-old NEMO^{LPC-KO} mice and littermate control mice (WT) (left panel) or IKK2^{LPC-KO} and WT mice (right panel) were analyzed by immunoblot with the indicated antibodies. Tubulin served as loading control.

(B) Protein extracts from primary hepatocytes isolated from NEMO^{LPC-KO}, IKK2^{LPC-KO}, and control mice were analyzed by immunoblot with the indicated antibodies.

(C and D) Macroscopic appearance of livers of NEMO^{LPC-KO} mice at 12 months of age. Arrows indicate large tumors.

(E and F) Normal macroscopic appearance of representative livers from a 12-month-old WT mouse (E) and IKK2^{LPC-KO} mouse (F).

(G–N) Representative hematoxylin/eosin (H/E)-stained liver sections showing normal histological architecture in a control mouse (G) and liver tumors in 12-month-old NEMO^{LPC-KO} mice (H–N). LGDN, low-grade dysplastic nodule; HGDN, high-grade dysplastic nodule (H). HCC, hepatocellular carcinoma (I–L and N). Arrows indicate the rims of tumors (I and J). Blue arrows indicate the rims of an area of broad trabecular growth of malignant tumor cells in four to six layers (L). Yellow arrows mark mitotic figures (N).

Spontaneous Liver Tumor Development in NEMO^{LPC-KO} Mice Is Preceded by Steatohepatitis

Hepatocellular carcinomas in humans frequently arise on the basis of chronic inflammation, whereas spontaneous development of malignant liver tumors in otherwise healthy livers is a rare event (Motola-Kuba et al., 2006; Okuda, 2000; Sherman, 2005). Therefore, we examined livers from NEMO^{LPC-KO}, IKK2^{LPC-KO}, and littermate control mice at different ages to assess whether these mice develop a liver phenotype already at younger age. Livers from 6-month-old NEMO^{LPC-KO} mice already displayed macroscopically visible nodules (Figures 2A–2C). On histological examination, focal areas of lipid accumulation and a variety of low-grade and high-grade dysplastic nodules with expansive growth were observed in livers from NEMO^{LPC-KO} mice at this stage (Figures 2D–2F). Furthermore, NEMO-deficient livers showed signs of steatosis with increased lipid deposition in hepatocytes (Figures 2G–2I), and hepatocyte ballooning (data not shown), a characteristic pathological feature seen in human nonalcoholic steatohepatitis (NASH) (Brunt, 2004).

Livers from 8-week-old NEMO^{LPC-KO} mice already showed signs of steatohepatitis characterized by immune cell infiltration into the liver parenchyma (Figures 3A and 3B) and steatosis (Figure 3C). Moreover, hepatocytes displayed characteristic features of large-cell dysplasia with strong anisokaryosis (Figures 3D and 3E), a condition also seen in chronic liver disease in humans, where it is associated with an increased risk for development of hepatocellular carcinoma (Libbrecht et al., 2001, 2005). Furthermore, Sirius red collagen staining revealed the presence of fibrosis in the liver of NEMO^{LPC-KO} mice (Figure S3), resembling the consequences of chronic inflammation and NASH in humans (Farrell and Larter, 2006) and also representing a risk factor for the development of hepatocellular carcinoma (Sherman, 2005). In contrast, mice lacking the IKK2 subunit in hepatocytes did not show histopathological alterations (Figure 3F). Therefore, conditional knockout

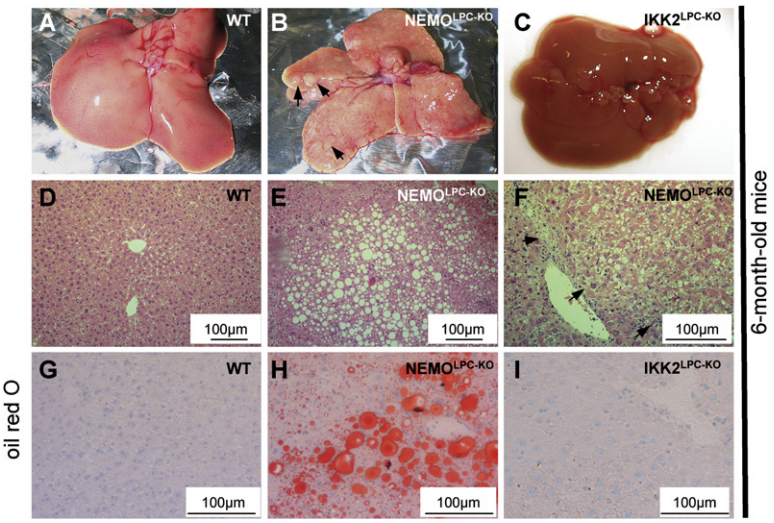

Figure 2. Macroscopic Nodules and NASH in 6-Month-Old NEMO^{LPC-KO} Mice

(A–C) Livers from 6-month-old control (A) and IKK2^{LPC-KO} mice are normal (C), while livers from NEMO^{LPC-KO} mice show macroscopically visible nodules (indicated by arrows) (B).

(D–F) Representative H/E-stained liver sections showing dysplastic nodules with vacuoles of accumulated fat in NEMO^{LPC-KO} (E and F) but not in control mice (D). Arrows indicate the rim of an expansively growing dysplastic nodule in (F).

(G–I) Representative oil-red-O-stained histological sections showing accumulation of lipids in NEMO^{LPC-KO} mice (H), but not in control (G) or IKK2^{LPC-KO} mice (I).

of NEMO in liver parenchymal cells leads to the spontaneous development of chronic hepatitis, steatosis, liver fibrosis, and HCC, a phenotype that resembles closely the sequence of events seen in human patients with nonalcoholic fatty liver disease (NAFLD) and NASH.

To further examine early stages of NASH development in NEMO^{LPC-KO} mice, we performed electron microscopy (EM) analysis on livers from 8-week-old mice. Mitochondria in hepatocytes in NEMO-deficient livers appeared swollen and displayed a reduction in mitochondrial crests compared to wild-type control tissue (Figures 3G and 3H), thus pointing toward a disturbance in mitochondrial function and oxidative metabolism. Moreover, large areas of irregularly shaped glycogen deposits could be detected in NEMO-deficient hepatocytes, compared to evenly distributed small areas of glycogen deposition in control livers (Figures 3G and 3H). Along with increased intracellular deposition of glycogen, NEMO^{LPC-KO} mice displayed a decrease in spontaneous serum glucose values compared to control mice (Figure 3I), whereas neither serum lipid levels nor serum insulin levels were elevated in these mice (Figure S4). These findings argue for a defect in hepatic glycogenolysis in NEMO^{LPC-KO} mice. It has been demonstrated previously that pharmacological inhibition of glycogenolysis in rats results in a stimulation of intrahepatic fat synthesis and development of hepatic steatosis

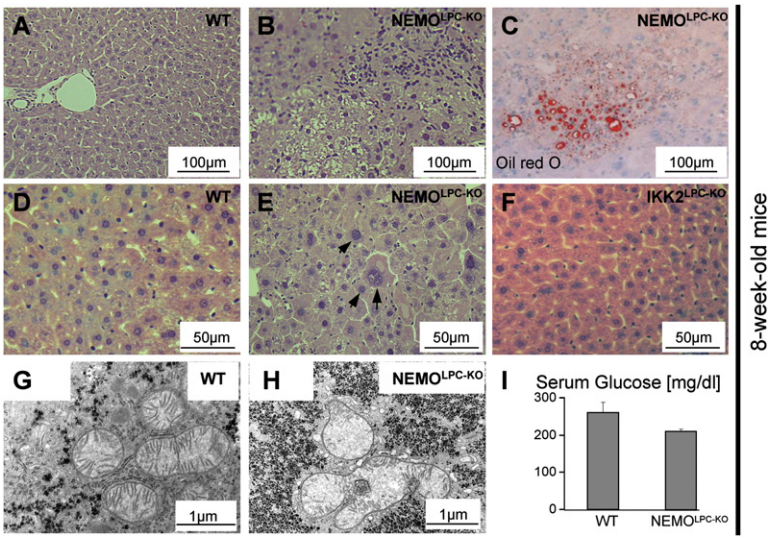

Figure 3. Spontaneous Hepatitis and Metabolic Alterations in NEMO^{LPC-KO} Mice at 8 Weeks of Age

(A and B) Histological analysis of liver sections from 8-week-old control (A) and NEMO^{LPC-KO} (B) mice reveal infiltration of mononuclear cells in the liver of NEMO^{LPC-KO} mice.

(C) Oil red O staining of liver sections from 8-week-old NEMO^{LPC-KO} mice shows areas of focal lipid accumulation.

(D–F) Representative H/E-stained histological sections of livers from 8-week-old mice show strong anisokaryosis (indicated by arrows) but normal nuclear-to-cytoplasmic ratio as signs of large-cell dysplasia in NEMO^{LPC-KO} mice (E) in contrast to normal histology in control (D) and IKK2^{LPC-KO} (F) mice.

(G and H) Representative electron microscopic (EM) pictures of mitochondria in the liver of control (G) and NEMO^{LPC-KO} mice (H). Notice the swelling and pleiomorphic form with strong reduction in mitochondrial crests along with large areas of abnormal glycogen deposition in NEMO^{LPC-KO} mice.

(I) Venous blood was drawn from six nonstarved mice per group between 10 a.m. and 11 a.m. from NEMO^{LPC-KO} and control mice. Spontaneous serum glucose was measured as indicated. Results are expressed as mean; error bars indicate standard error of the mean (SEM).

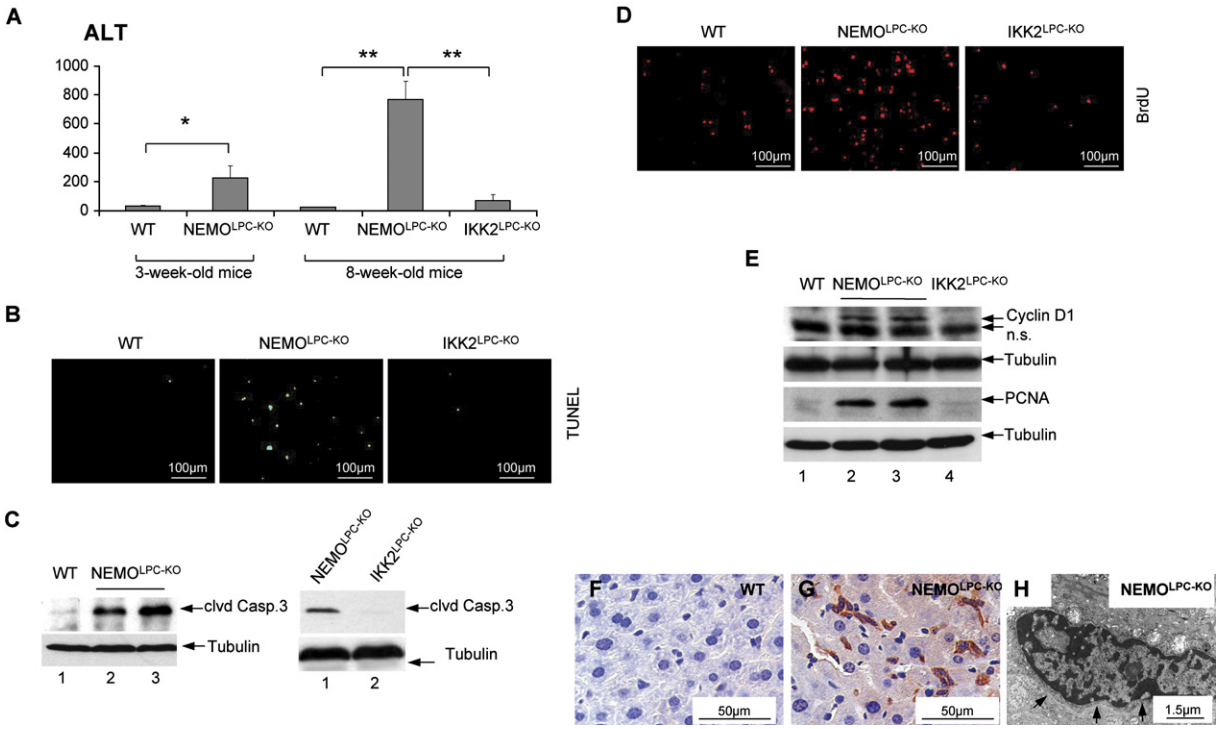

Figure 4. Enhanced Cell Death and Cell-Cycle Activation in NEMO^{LPC-KO} Mice

(A) Circulating ALT levels in serum from mice at 3 weeks and 8 weeks of age as indicated. *$p < 0.05$ compared to control mice. **$p < 0.01$ compared to control and IKK2^{LPC-KO} mice. Results are expressed as mean; error bars indicate SEM.

(B) Representative TUNEL staining of liver sections from 8-week-old male mice showing increased apoptosis in NEMO^{LPC-KO} mice compared to wild-type and IKK2^{LPC-KO} mice.

(C) Immunoblot analysis on whole-liver extracts from 8-week-old NEMO^{LPC-KO}, IKK2^{LPC-KO}, and wild-type control mice using an antibody that specifically detects the cleaved form of caspase-3 or tubulin as loading control.

(D) Representative BrdU staining on liver samples from 8-week-old NEMO^{LPC-KO}, IKK2^{LPC-KO}, and control mice that had been pulse labeled with BrdU every 8 hr for 2 days prior to sacrificing.

(E) Immunoblot analysis on whole-liver extracts from 8-week-old mice using antibodies against Cyclin D1, PCNA, or tubulin as loading control.

(F and G) Immunohistochemical staining of liver sections from 8-week-old NEMO^{LPC-KO} and control mice revealing strong activation of hepatic progenitor cells (oval cells) in NEMO^{LPC-KO} mice (F).

(H) Representative EM picture of an oval cell in NEMO^{LPC-KO}. The arrow indicates the basal membrane as one of the specific features of a progenitor cell in the liver.

(Bandsma et al., 2001; Herling et al., 1999), suggesting that a disturbance in hepatic carbohydrate metabolism might be the initial event in the development of fatty liver disease in NEMO^{LPC-KO} mice.

Increased Hepatocyte Apoptosis and Regeneration in the Liver of NEMO^{LPC-KO} Mice

The finding that young NEMO^{LPC-KO} mice show liver inflammation and steatosis prompted us to examine further the early stages of this phenotype. At 3 weeks of age, NEMO^{LPC-KO} mice displayed a considerable elevation of alanine aminotransferase (ALT) in the serum, indicating the presence of hepatocyte damage, and ALT levels were further increased at 8 weeks (Figure 4A). Furthermore, 8-week-old NEMO^{LPC-KO} mice showed an increased number of TUNEL-positive cells and activation of caspase-3 in the liver compared to control and IKK2^{LPC-KO} animals (Figures 4B and 4C). Therefore, increased apoptotic death of hepatocytes occurs spontaneously in the liver of NEMO^{LPC-KO} mice and is already apparent at 3 weeks of age. In parallel with increased cell death, we detected increased proliferation in the liver of NEMO^{LPC-KO} mice, as demonstrated by an elevated number of cells incorporating BrdU and by the upregulation of Cyclin D1 and PCNA expression, two markers indicating cell-cycle activation (Figures 4D–4E).

Chronic inflammation can impose restrictions on the proliferative capacity of hepatocytes, leading to impaired liver regeneration (Marshall et al., 2005). Oval cells are bipotential hepatic progenitor cells with a long-term repopulating potential that are activated in many chronic liver diseases where increased hepatocyte loss needs to be compensated by enhanced liver regeneration (Alison and Lovell, 2005). Immunohistochemical staining revealed strong activation of oval cells in the liver of 8-week-old NEMO^{LPC-KO} mice compared to controls (Figures 4F and 4G). Furthermore, EM analysis confirmed the increased presence of activated progenitor cells in the liver of these

mice (Figure 4H). Taken together, these findings suggest that chronic spontaneous hepatocyte death induces a regenerative response with compensatory hepatocyte proliferation and activation of hepatic progenitor cells in NEMO^{LPC-KO} mice, which may form the basis for the development of liver cancer in these mice.

Deletion of NEMO Completely Blocks NF-κB Activation and Sensitizes the Liver to LPS-Induced Toxicity

The finding that NEMO^{LPC-KO} but not IKK2^{LPC-KO} mice develop spontaneous liver disease and cancer prompted us to investigate further the effects of NEMO versus IKK2 deletion in the liver, in particular with regards to NF-κB activation and protection from cytokine-induced toxicity. TNF administration in vivo failed to induce NF-κB activation in the liver of adult NEMO^{LPC-KO} mice (Figure 5A). Moreover, NEMO^{LPC-KO} mice showed complete inhibition of NF-κB activation upon injection of lipopolysaccharide (LPS) (Figure 5B), which acts as a potent inducer of endogenous TNF and other cytokines (Pasparakis et al., 1996; Pfeffer et al., 1993). Under the same treatment, considerable NF-κB activation was detected in the liver of IKK2^{LPC-KO} mice, showing that *Ikk2* deletion does not result in complete NF-κB inhibition in response to LPS (Figure 5C). TNF stimulation of primary hepatocytes confirmed that NEMO knockout blocks completely IκBα degradation, while substantial IκBα degradation occurs in the absence of IKK2 (Figure 5D). Therefore, NEMO ablation leads to complete inhibition of NF-κB activation by LPS and TNF in the liver, while considerable NF-κB activity is retained in the absence of IKK2, presumably due to compensatory signaling by IKK1.

Consistent with the lack of NF-κB activation, NEMO^{LPC-KO} mice developed massive hepatocyte apoptosis and fulminant liver failure upon LPS challenge (Figures 5E and 5F), demonstrating that NF-κB activation is essential to protect the adult liver from TNF-induced apoptosis. LPS administration did not cause substantial liver damage and hepatocyte apoptosis in the liver of IKK2^{LPC-KO} mice (Figures 5E and 5F), consistent with the considerable induction of NF-κB activity in the absence of IKK2. This finding is in accordance with previous results, obtained using either the same IKK2^{LPC-KO} mice employed in this report (Luedde et al., 2005) or a different hepatocyte-specific IKK2 knockout strain (Maeda et al., 2003), showing that deletion of IKK2 in liver parenchymal cells does not sensitize the liver to LPS/TNF challenge. Taken together, these results demonstrate that deletion of NEMO, but not IKK2, completely blocks NF-κB activation in hepatocytes and uncovers the essential role of NF-κB to protect the adult mouse liver from TNF-induced toxicity.

Increased Cytokine Expression, JNK Activation, and Impaired Antiapoptotic Gene Expression in NEMO^{LPC-KO} Mice

To further investigate the role of inflammation in the development of hepatitis in NEMO^{LPC-KO}, mice we analyzed the expression of proinflammatory mediators in the liver. We found upregulation of TNF, IL-6, IL-1β, and RANTES in the liver of NEMO^{LPC-KO} mice (Figure 6A), suggesting that increased expression of proinflammatory cytokines and chemokines is implicated in the development of hepatitis in these mice. These cytokines are likely to be produced by Kupffer cells, which are the main source of cytokines in the liver (Ramadori and Armbrust, 2001). As Kupffer cells are not targeted by the Alfp-Cre transgene (Kellendonk et al., 2000; Luedde et al., 2005), they express NEMO and have full capacity to activate NF-κB and produce proinflammatory mediators. Consistently, immunohistochemical analysis identified nonparenchymal liver cells as the major source of TNF in NEMO^{LPC-KO} mice (Figure 6B). Hepatocyte death activates Kupffer cells in models of chronic liver injury (Canbay et al., 2005), suggesting that increased spontaneous death of NF-κB-deficient parenchymal cells in NEMO^{LPC-KO} mice might induce the expression of cytokines and chemokines from Kupffer cells.

We aimed to analyze further the molecular mechanisms that lead to spontaneous hepatocyte death in NEMO^{LPC-KO} mice. JNK activation has been suggested as an important mediator of TNF-induced cell death in the liver (Schwabe and Brenner, 2006). Analysis of JNK phosphorylation revealed constitutive JNK activation in the liver of NEMO^{LPC-KO}, but not in control or IKK2^{LPC-KO} mice (Figure 6C), suggesting that the increased cell death of NEMO-deficient hepatocytes might be caused by persistent JNK activity. Analysis of the expression of NF-κB target genes known to have antiapoptotic and antioxidant functions revealed that XIAP, cIAP-1, GADD45α, SOD1, and SOD2 were downregulated in the liver of NEMO^{LPC-KO} mice (Figure 6D). In contrast, the expression of Bax, a Bcl-2 family member with proapoptotic function (Festjens et al., 2004), was upregulated in the NEMO-deficient liver (Figure 6D). Moreover, immunoblot analysis showed that the expression of Bcl-2 was unaffected, while the majority of Bax protein was processed into a lower-molecular-weight form in the liver of NEMO^{LPC-KO} mice (Figure 6E). Previous studies suggested that inhibition of NF-κB leads to increased expression of Bax (Bentires-Alj et al., 2001), and that an N-terminally cleaved 18 kDa form of Bax is a more potent inducer of cell death acting independently of the protecting function of Bcl-2 (Gao and Dou, 2000). Furthermore, oxidative stress-induced apoptosis in hepatocytes can lead to N-terminal Bax cleavage (Tamura et al., 2003), again pointing toward an important role for oxidative stress as mediator of cell death in NEMO^{LPC-KO} mice.

Antioxidant Treatment Prevents the Development of Steatohepatitis in NEMO^{LPC-KO} Mice

To evaluate the contribution of oxidative stress to the pathogenesis of liver disease in NEMO^{LPC-KO} mice, we placed a group of mice on a diet supplemented with the antioxidant butylated hydroxyanisole (BHA) starting at 4 weeks of age and followed them until they were 10 weeks old. NEMO^{LPC-KO} mice on the BHA diet showed an immediate and striking improvement of the hepatitis phenotype, as

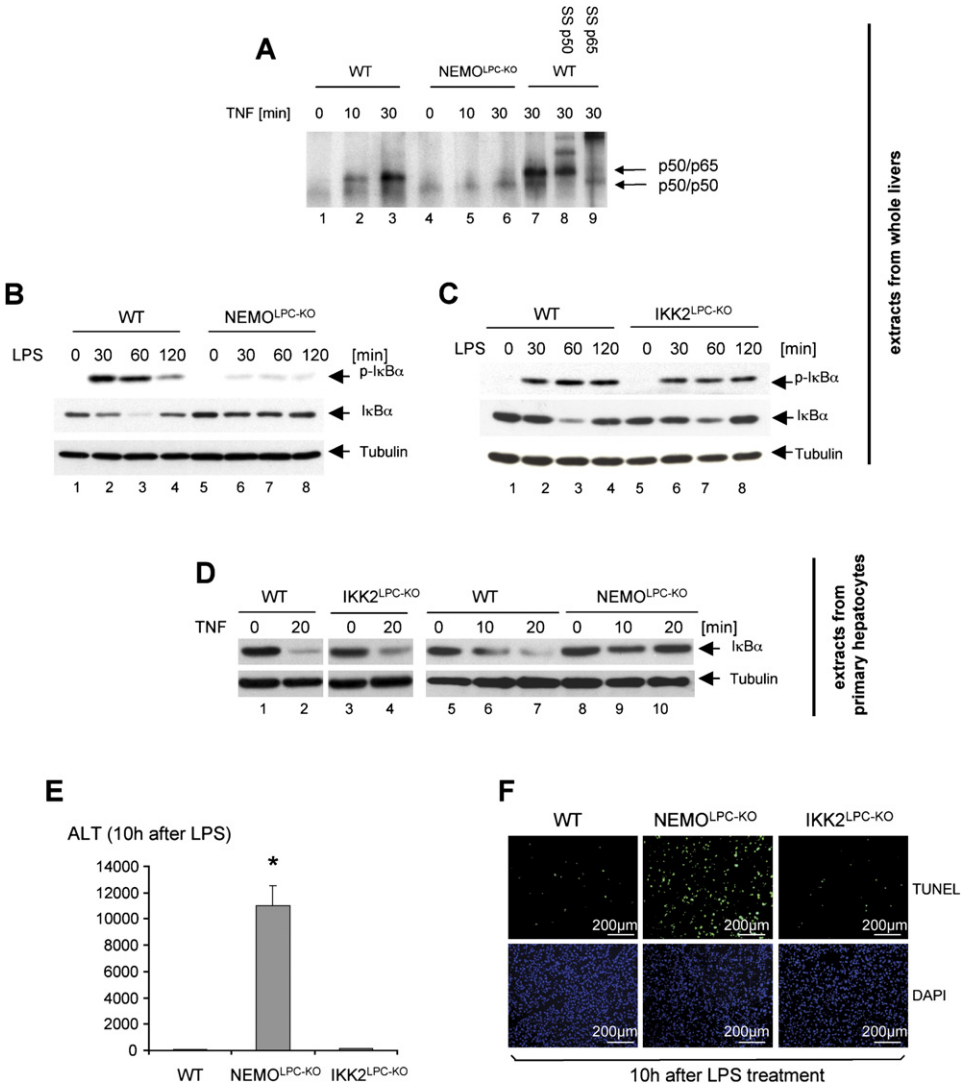

Figure 5. Ablation of NEMO Specifically in Liver Parenchymal Cells Blocks NF-κB Activation and Sensitizes the Liver to LPS-Induced Toxicity

(A) Nuclear protein extracts were prepared from the liver of NEMO^{LPC-KO} and wild-type mice at the indicated time points after TNF stimulation and were subjected to a gel retardation assay with an NF-κB consensus probe to measure NF-κB DNA-binding activity as described under Experimental Procedures. In lanes 8 and 9, antibodies for the NF-κB subunits p50 or p65 were added as indicated to identify the respective NF-κB dimers by supershifting.

(B and C) IκBα phosphorylation and degradation were assessed by immunoblot analysis of liver protein extracts from NEMO^{LPC-KO} (B), IKK2^{LPC-KO} (C), and their respective littermate control mice at the indicated time points after LPS administration using antibodies against phosphorylated IκBα, total IκBα, or tubulin as loading control.

(D) Primary hepatocytes from the indicated mouse lines were stimulated with murine recombinant TNF for the indicated time points, and degradation of IκBα was assessed by immunoblot.

(E) Liver damage 10 hr after LPS stimulation in NEMO^{LPC-KO}, IKK2^{LPC-KO}, and control mice (WT) was assessed by analysis of serum ALT levels. *$p < 0.01$ compared to control and IKK2^{LPC-KO} mice. Results are expressed as mean; error bars indicate SEM.

(F) Representative TUNEL staining of liver sections 10 hr after LPS stimulation showing massive apoptosis in NEMO^{LPC-KO} but not in IKK2^{LPC-KO} or wild-type mice. Nuclei were visualized by DAPI staining.

shown by a drop of serum ALT to almost normal levels (Figure 7A). Furthermore, histological analysis of the liver from these mice showed a significant improvement of the pathological changes with a strong reduction of spontaneous hepatocyte apoptosis and also of inflammation and anisokaryosis compared to untreated NEMO^{LPC-KO} mice (Figures 7B and 7C). In addition, BHA treatment led to a strong reduction in JNK activation and normalized the increased expression of Bax in the liver of NEMO^{LPC-KO} mice (Figures 7D–7E). Electron microscopy revealed a normalization of mitochondrial structure along with signs of increased mitochondrial biogenesis as shown by dividing mitochondria, and also normalization of glycogen distribution in the liver from BHA-treated mice (Figure 7F).

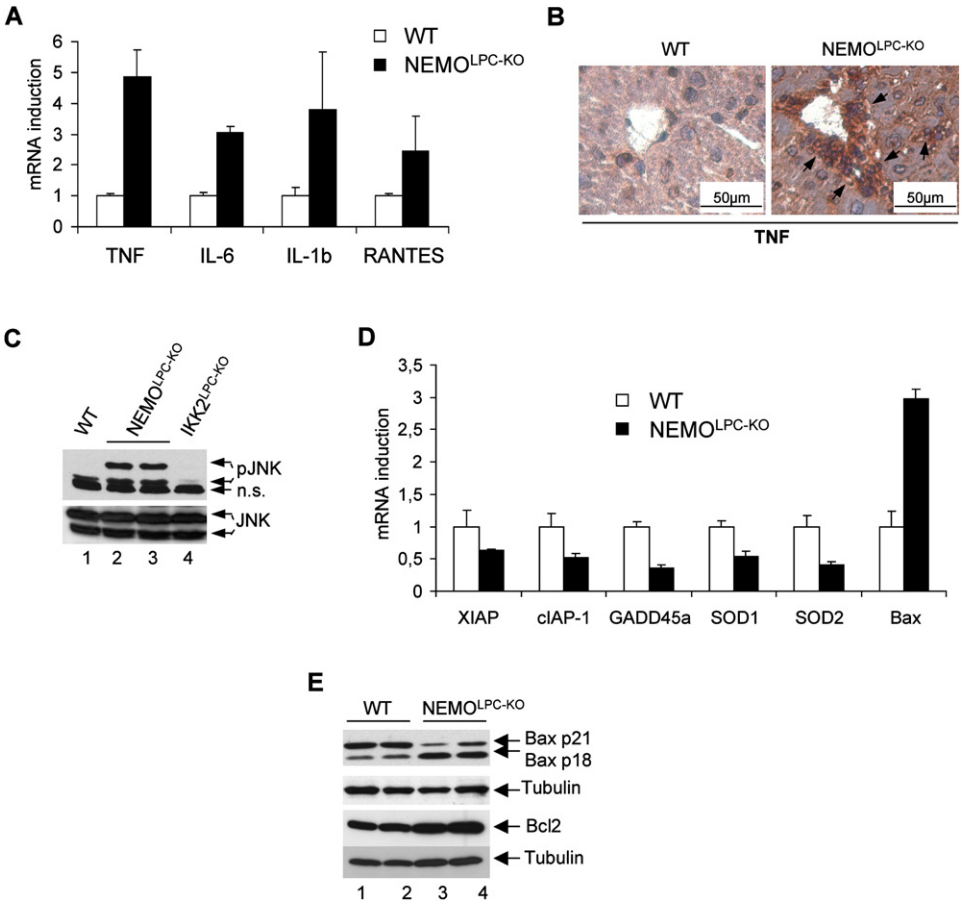

Figure 6. Increased Cytokine Expression, JNK Activation, and Impaired Antiapoptotic Gene Transcription in NEMO^{LPC-KO} Mice

(A) Quantitative RT-PCR analysis of cytokine mRNA levels in the liver of 8-week-old mice. Results are expressed as mean; error bars indicate SEM.

(B) Immunohistochemical staining for TNF reveals TNF expression mainly in nonparenchymal liver cells in NEMO^{LPC-KO} mice.

(C) Liver protein extracts from 8-week-old NEMO^{LPC-KO} and control mice were prepared and subjected to immunoblot using antibodies detecting either the phosphorylated or the total forms of p46 and p54 JNK.

(D) Quantitative RT-PCR analysis of the mRNA levels of the indicated genes in the liver of 5-week-old NEMO^{LPC-KO} and control mice. Values are mean ± SEM from three mice per group.

(E) Immunoblot analysis of liver protein extracts from 8-week-old NEMO^{LPC-KO} and control mice using antibodies against Bax, Bcl-2, or tubulin as loading control. The Bax antibody detects two isoforms of Bax, with a shorter, cleaved form as the predominant form in NEMO^{LPC-KO} mice.

Furthermore, no signs of steatosis or increased lipid deposition were seen after 6 weeks of BHA treatment (Figure 7G). These findings argue that the development of steatosis is a secondary event caused by oxidative stress-dependent mechanisms. Therefore, treatment with the antioxidant BHA normalized all aspects of the liver disease developing in NEMO^{LPC-KO} mice, demonstrating that increased oxidative stress plays a critical role in the induction of sustained JNK activation leading to hepatocyte death and steatohepatitis in this model.

The Development of Steatohepatitis in NEMO^{LPC-KO} Mice Depends on FADD-Mediated Hepatocyte Apoptosis

The increased expression of cytokines such as TNF, which are known to induce apoptosis in liver parenchymal cells under certain circumstances (Luedde et al., 2002), prompted us to investigate whether the increased oxidative stress, JNK activity, and cell death in the liver of NEMO^{LPC-KO} mice is induced by death-receptor signaling. FADD is an adaptor molecule that is essential for caspase-8 activation and induction of cell death downstream of TNFRI and Fas (Strasser and Newton, 1999). To investigate in vivo the role of FADD in the induction of liver apoptosis, we generated mice with liver parenchymal cell-specific FADD knockout (FADD^{LPC-KO}) by crossing mice with a loxP-flanked *Fadd* allele (G.v.L. and M.P, unpublished data) with the *Alfp*-Cre transgenic mice. In order to test whether the increased hepatocyte death in the NEMO^{LPC-KO} mice depends on death receptor-induced apoptosis, we interbred the NEMO^{LPC-KO} mice with the FADD^{LPC-KO} mice to generate mice lacking both NEMO and FADD in the liver (NEMO/FADD^{LPC-KO}) (Figure 8A). The double NEMO/FADD^{LPC-KO} mice were protected from LPS-induced hepatocyte apoptosis compared to NEMO^{LPC-KO} mice (Figures 8B–8D), demonstrating that

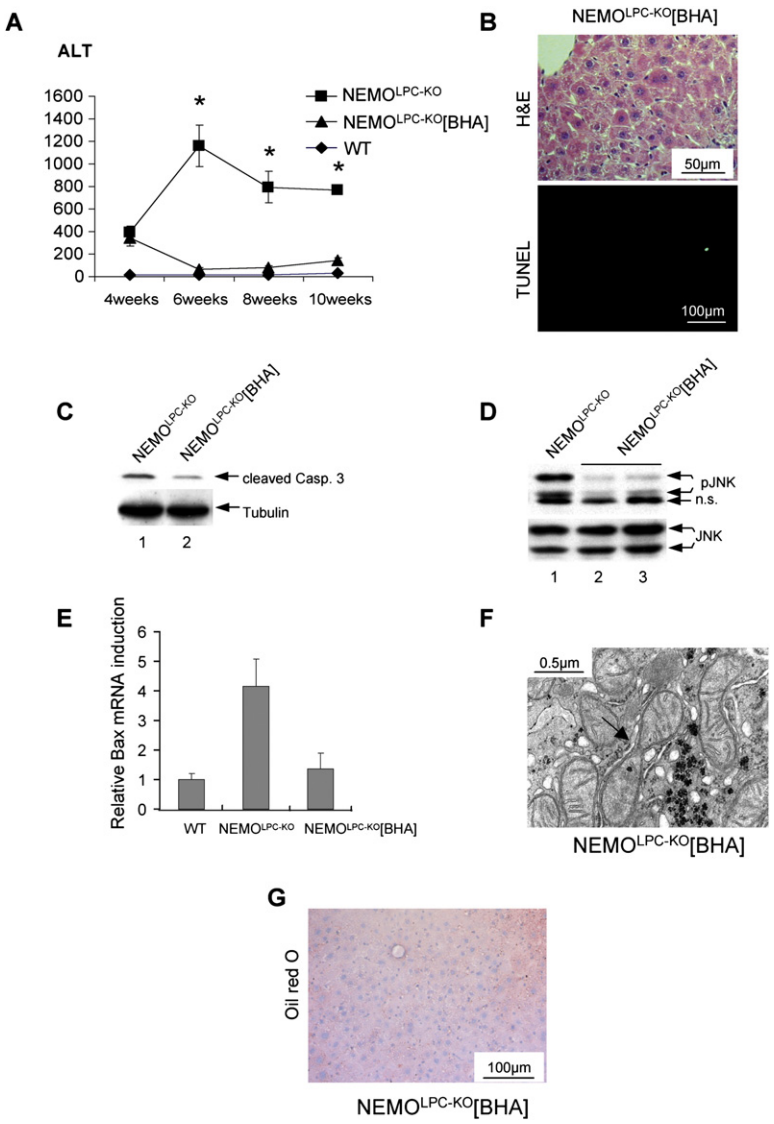

Figure 7. Role of Oxidative Stress in Development of Hepatitis and NASH in NEMO^{LPC-KO} Mice

(A) Serum ALT levels in a group of NEMO^{LPC-KO} mice receiving a diet supplemented with 0.7% BHA starting at 4 weeks of age compared with NEMO^{LPC-KO} and control mice on a normal diet. *p < 0.05 compared to NEMO^{LPC-KO} mice on normal diet. Results are expressed as mean; error bars indicate SEM.

(B) Representative H&E staining (upper panel) and TUNEL staining (lower panel) from NEMO^{LPC-KO} mice on a diet supplemented with BHA at 10 weeks of age. (Compare to NEMO^{LPC-KO} mice on normal diet at the same age [Figures 3E and 4B].)

(C) Immunoblot analysis of liver extracts from 10-week-old mice using antibodies against cleaved caspase-3 or tubulin as loading control.

(D) Immunoblot analysis with antibodies detecting specifically the phosphorylated form of JNK or total JNK on whole-liver extracts from NEMO^{LPC-KO} mice on normal diet (lane1) and NEMO^{LPC-KO} mice on BHA diet (lanes 2 and 3).

(E) Quantitative RT-PCR analysis of Bax mRNA expression in livers from control mice, NEMO^{LPC-KO} mice on normal diet, and NEMO^{LPC-KO} mice on BHA diet. Results are expressed as mean; error bars indicate SEM.

(F) Representative EM analysis of mitochondria in livers from NEMO^{LPC-KO} mice treated for 6 weeks with BHA, showing normalization of mitochondrial structure and normal distribution of glycogen. The arrow indicates an area of mitochondrial division as a sign of biogenesis of mitochondria upon antioxidant treatment.

(G) Representative oil red O staining on a liver slide from 10-week-old NEMO^{LPC-KO} mice treated for 6 weeks with the antioxidant BHA. Note that no focal lipid accumulation was detected in the mice at this stage (compare to Figure 3C).

FADD deficiency blocks death receptor-induced killing of NF-κB-deficient hepatocytes. Although hepatocytes lacking both NEMO and FADD were protected from apoptosis, we detected sustained JNK activation in the liver of double NEMO/FADD^{LPC-KO} mice upon LPS injection (Figure S5A). These experiments provide an in vivo genetic proof that FADD-dependent caspase-8 activation is essential for the induction of cell death downstream of oxidative stress-induced sustained JNK activation.

We then analyzed whether FADD deficiency also neutralized the spontaneous hepatocyte apoptosis and hepatitis in NEMO^{LPC-KO} mice. Indeed, double NEMO/FADD^{LPC-KO} mice showed strongly decreased spontaneous serum ALT values compared to NEMO^{LPC-KO} mice (Figure 8E), together with a clear improvement in liver histology marked by the complete disappearance of inflammation, decreased spontaneous apoptosis, and absence of anisokaryosis at the age of 8 weeks (Figures 8F and 8G). Therefore, the spontaneous hepatocyte cell death and hepatitis in NEMO^{LPC-KO} mice is caused by FADD-dependent signaling downstream of death receptors such as Fas and TNFRI. Despite the rescue of hepatocyte apoptosis, double NEMO/FADD^{LPC-KO} mice showed increased spontaneous JNK activity in the liver similarly to NEMO^{LPC-KO} mice, in contrast to mice treated with BHA, where the sustained JNK activation was abolished (Figure 8H). In addition to rescuing hepatocyte death, FADD deficiency also inhibited the increased proliferation observed in the liver of NEMO^{LPC-KO} mice, as shown by the reduced expression of cyclin D1 and PCNA in the liver of double NEMO/FADD^{LPC-KO} mice (Figure 8I). This finding shows that the increased proliferation in the liver of NEMO^{LPC-KO} mice is a secondary event induced in response to the death of hepatocytes. In addition, NEMO/FADD^{LPC-KO} mice at the age of 4 months did not show

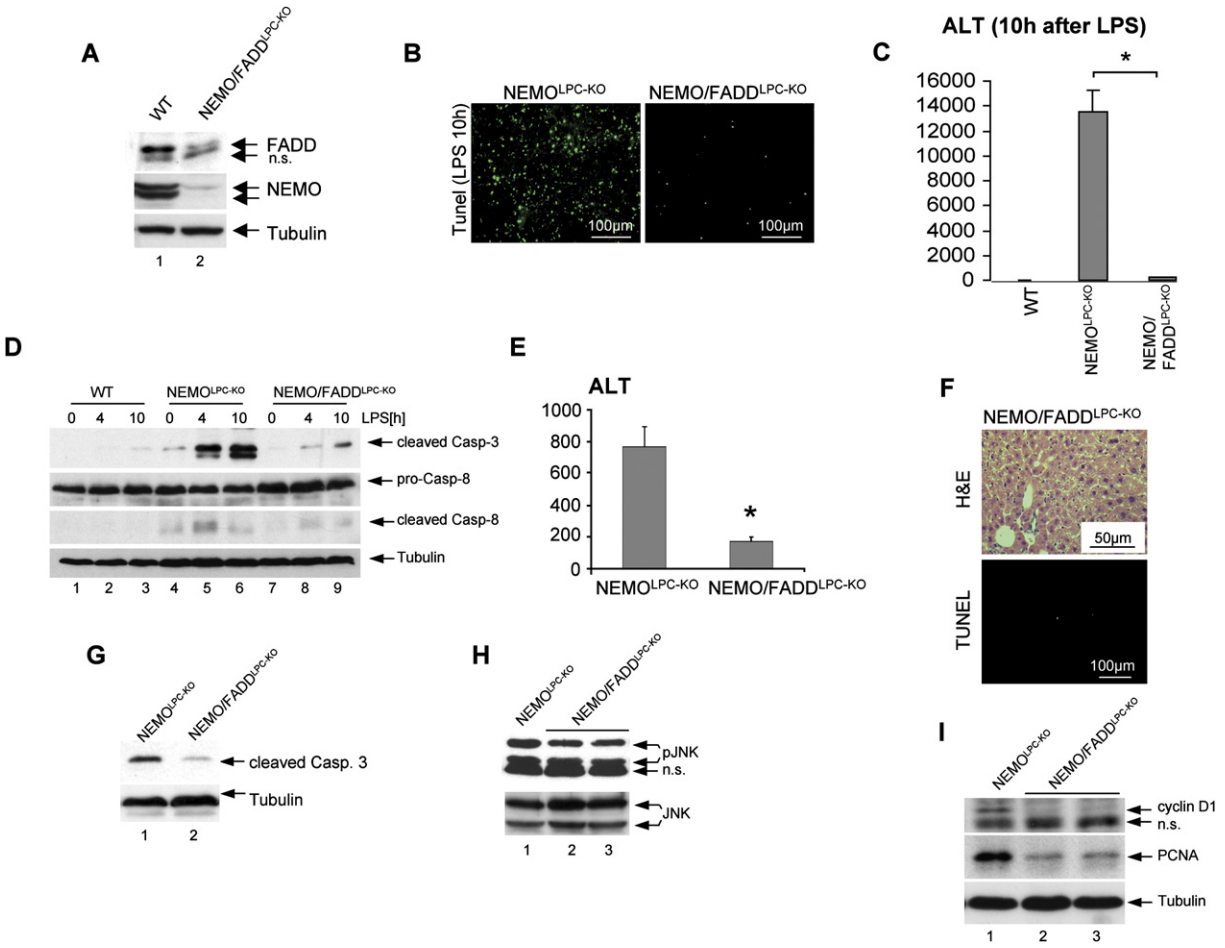

Figure 8. Role of Death-Receptor Signaling in Hepatitis in NEMO^{LPC-KO} Mice

(A) Efficient ablation of both NEMO and FADD in the liver of double NEMO/FADD^{LPC-KO} mice, as shown by immunoblot of liver protein extracts with the indicated antibodies.

(B) Representative TUNEL staining on liver slides from mice with the indicated genotypes 10 hr after LPS stimulation.

(C) Measurement of serum ALT levels 10 hr after LPS injection shows protection of NEMO/FADD^{LPC-KO} mice from liver damage. *$p < 0.01$. Results are expressed as mean; error bars indicate SEM.

(D) Immunoblot analysis on liver protein extracts from mice with the indicated genotypes at different time points after LPS treatment, using antibodies detecting the cleaved form of caspase-3, both pro-caspase-8 and cleaved caspase-8, and tubulin as loading control.

(E) Measurement of serum ALT shows significantly reduced spontaneous liver injury in NEMO/FADD^{LPC-KO} mice compared NEMO^{LPC-KO} animals at 8 weeks of age. *$p < 0.05$ compared to NEMO^{LPC-KO} mice. Results are expressed as mean; error bars indicate SEM.

(F) Representative H&E staining (upper panel) and TUNEL staining (lower panel) on slides of livers from mice at 8 weeks of age.

(G) Immunoblots on extracts from 8-week-old NEMO^{LPC-KO} and NEMO/FADD^{LPC-KO} mice using antibodies against cleaved caspase-3 or tubulin as loading control.

(H) Immunoblots with antibodies detecting specifically the phosphorylated form of JNK or total JNK as loading control.

(I) Immunoblots using extracts from 8-week-old NEMO^{LPC-KO} and NEMO/FADD^{LPC-KO} mice with antibodies against cyclin D1, PCNA, and tubulin as loading control.

focal lipid accumulation, which was already apparent in NEMO^{LPC-KO} mice at the age of 8 weeks (Figure S5B). This result suggests that the increased fat deposition in the liver of NEMO^{LPC-KO} mice is a secondary consequence of the chronic hepatitis associated with inflammation and oxidative stress, rather than a primary metabolic defect. Taken together, these findings show that FADD-dependent death of NEMO-deficient hepatocytes is an essential upstream event that triggers the development of steatohepatitis in NEMO^{LPC-KO} mice.

DISCUSSION

Here we show that ablation of NEMO/IKKγ in liver parenchymal cells caused the spontaneous development of hepatocellular carcinoma in mice. These findings revealed a physiological function of NF-κB in protecting the liver from cancer, identifying NEMO as a tumor suppressor in the liver. The tumors developed in the context of chronic hepatitis resembling human nonalcoholic fatty liver disease (NAFLD) and NASH. A link between NASH and

HCC in humans has only recently become apparent, although the extent of this association remains unclear (Brunt, 2004; Farrell and Larter, 2006). Our findings that steatotic hepatitis and HCC developed with 100% penetrance in NEMO^{LPC-KO} mice show that the NASH-like hepatitis phenotype predisposes to liver carcinogenesis, suggesting that also in humans NASH may constitute a critical risk factor for HCC development. Given that NAFLD and NASH are expected to account for an increasing percentage of chronic liver diseases leading to cirrhosis and liver cancer in Western countries (Farrell and Larter, 2006), the NEMO^{LPC-KO} mice represent an animal model that may be valuable to further characterize the molecular mechanisms leading to cancer development in the context of NASH.

Using genetic and pharmacological in vivo analysis, we demonstrated that the FADD-mediated and oxidative stress-dependent death of NF-κB-deficient hepatocytes was the critical pathogenic step that triggered chronic liver disease and cancer in this model. These results shed light on the controversial discussion about the function of NF-κB in the development of HCC and suggest the following model for the development of liver tumors in the NEMO^{LPC-KO} mice: NEMO-deficient hepatocytes undergo apoptosis in response to FADD-mediated and oxidative stress-dependent death-receptor signaling. Hepatocyte death triggers inflammation and a regenerative response in the liver with reactive proliferation of hepatocytes. In this chronic state of liver inflammation, apoptosis, and regeneration, hepatocytes proliferating under conditions of increased oxidative stress may accumulate mutations leading to dysplasia and eventually to tumor development. Apoptosis is generally considered as a mechanism preventing tumor development, and evasion of apoptotic cell death is considered a classic cellular feature contributing to cancer (Hanahan and Weinberg, 2000). In this context, NF-κB activation is generally considered as a survival signal allowing tumor cells to escape apoptosis, and thus NF-κB inhibition is expected to have antioncogenic effects. Our results, on the other hand, demonstrate that in the liver NF-κB inhibition promotes hepatocarcinogenesis by sensitizing hepatocytes to spontaneous apoptosis. This apparent contradiction can be explained by the unique features of the liver, which has the capacity to regenerate upon injury through the compensatory proliferation of hepatocytes. Liver responses to injury are determined by the unique interplay between parenchymal and nonparenchymal liver cells, with hepatocyte death inducing activation of Kupffer cells that in turn produce cytokines to promote regeneration. Therefore, in a tissue such as the liver, susceptibility to apoptosis as seen in the NEMO^{LPC-KO} mouse may lead to a chronic state of hepatocyte death and regenerative proliferation, which constitutes a risk factor for cancer development.

Oval cells—hepatocyte progenitor cells located in the periphery of the biliary tract—represent a constant source to restore the pool of hepatocytes in the liver, and their potential involvement in liver tumor development in both humans and in animal models has recently raised increasing interest (Alison and Lovell, 2005; Fang et al., 2004; Libbrecht et al., 2005). Furthermore, a recent study identified a subtype of hepatocellular carcinomas related to hepatic progenitor cells that was linked with a poor prognosis (Lee et al., 2006). We found strong activation of oval cells in NEMO^{LPC-KO} mice, suggesting that the mobilization of the stem-cell pool of the liver is critical to provide a constant cellular source to compensate for the loss of parenchymal cells. However, at this stage it remains unclear whether the tumors developing in the NEMO-deficient livers are, at least in part, derived from progenitor cells.

Deletion of *Ikk2* does not lead to spontaneous liver pathology. IKK2 in contrast to NEMO is a kinase and thus might have other substrates than IκBα, whereas NEMO so far has only been linked to NF-κB activity, meaning that loss of NEMO and IKK2 cannot be equated. However, our results suggest that the difference between the NEMO^{LPC-KO} and IKK2^{LPC-KO} mice lies in the differential effect of these two knockouts on inhibiting NF-κB activation and antiapoptotic function. In contrast to NEMO^{LPC-KO} mice, IKK2^{LPC-KO} animals are not sensitive to LPS- or TNF-induced liver damage, showing that the level of NF-κB inhibition achieved by *Ikk2* deletion is not sufficient to sensitize hepatocytes to cytokine-induced toxicity. Therefore, a critical threshold of NF-κB activity determines the ability of liver parenchymal cells to survive during adult life, and inhibition of NF-κB below this threshold, achieved here by deletion of NEMO, renders hepatocytes dramatically sensitive to death receptor-induced apoptosis resulting in chronic hepatitis. Although the ligand-receptor pair(s) that play a critical role in inducing spontaneous hepatocyte apoptosis in NEMO^{LPC-KO} mice are not known at present, it is likely that hepatocyte death is initiated by small amounts of cytokines produced normally in mice living in a nonsterile surrounding. These cytokines may be expressed by innate immune cells that are activated through Toll-like receptors in response to contact with bacteria or bacterial products, which originate from the large intestine and are transported to the liver via the portal circulation, where they can activate hepatic Kupffer cells to produce inflammatory cytokines such as TNF (Enomoto et al., 2002). As the mice reported in this study were not kept under germ-free conditions, it is possible that bacteria that are apparently not pathogenic for wild-type or IKK2^{LPC-KO} mice are transformed into inducers of chronic liver disease and HCC in NEMO^{LPC-KO} mice due to the extreme sensitivity of NEMO-deficient hepatocytes to cytokine-induced cell death. Future experiments on germ-free animals will be required to address experimentally this hypothesis.

Mutations in the X-linked human *NEMO* gene cause two distinct genetic diseases, hypohydrotic ectodermal dysplasia with immune deficiency (HED-ID) and incontinentia pigmenti (IP), in humans (Courtois, 2005), but have not been associated with liver cancer. HED-ID is caused by hypomorphic NEMO mutations, which do not completely abolish but rather reduce NF-κB activation, resulting in impaired skin appendage development and severe immune deficiency. The lack of a liver defect in HED-ID

patients could be explained by the incomplete inhibition of NF-κB and by the presence of the mutation in all cells, in contrast to the NEMO^{LPC-KO} mice, where NF-κB-deficient hepatocytes are killed by cytokines expressed by cells expressing NEMO. IP is caused by mutations disrupting the human *NEMO* gene. Male IP patients die in utero, whereas heterozygous female patients survive and display a range of clinical phenotypes caused by the mosaic presence of NEMO-deficient cells in multiple tissues. Liver complications are not usually reported in those female IP patients, although there is one such report in the literature (Oberti et al., 1997). The most likely explanation for this is that, due to their extreme sensitivity to apoptosis, the NEMO-deficient cells quickly disappear from the mosaic livers and are replaced by wild-type cells. This is likely to happen during embryonic development, based on results obtained from *Nemo* knockout mouse models (Makris et al., 2000; Rudolph et al., 2000; Schmidt-Supprian et al., 2000). Therefore, adult IP patients would be expected to have only NEMO-expressing hepatocytes and would not show any liver phenotype. This hypothesis is strongly supported by a case report about a female infant born to a mother with IP and a father with hemophilia A, who showed a highly skewed pattern of X inactivation and manifested both disorders (Coleman et al., 1993).

The results reported in this study raise important considerations for pharmacological therapies targeting the IKK complex in human patients, which has been suggested as a powerful approach to treat inflammatory and other disorders (Burke, 2003). Our experiments show that complete inhibition of IKK activity in hepatocytes might be detrimental and might result in liver disease and even liver cancer upon long-term treatment. This might be particularly relevant for pharmacological inhibitors that would target the regulatory function of NEMO rather than the activity of IKK2. On the other hand, depending on pharmacokinetic properties, pharmacological inhibition of the IKK complex targeting all cells might lead to a different outcome than our hepatocyte-specific genetic approach, by neutralizing the expression of cytokines from effector cells and thus eliminating the trigger causing the death of NF-κB-deficient hepatocytes. In any case, our findings highlight the need for extensive research on the potential detrimental consequences of long-term NF-κB inhibition.

EXPERIMENTAL PROCEDURES

Generation of Conditional Knockout Mice for NEMO, IKK2, and NEMO/FADD

Mice carrying loxP-site-flanked (floxed [Fl]) *Nemo* (*Nemo*^{Fl}) and *Ikk2* alleles (*Ikk2*^{Fl}) were described previously (Pasparakis et al., 2002; Schmidt-Supprian et al., 2000). *Nemo*^{FL} and *Ikk2*^{FL} mice were crossed to *Alfp*-Cre transgenic mice (Kellendonk et al., 2000) to generate a parenchymal liver cell-specific knockout of the respective gene (NEMO^{LPC-KO} and IKK2^{LPC-KO}). NEMO^{LPC-KO} mice were crossed to *Fadd*^{Fl} mice (G.V.L. and M.P., unpublished data) for a conditional double-knockout of both *Nemo* and *Fadd* (NEMO/FADD^{LPC-KO}) in liver parenchymal cells. In all experiments, littermates carrying the respective loxP-flanked alleles but lacking expression of Cre recombinase were used as wild-type (WT) controls. All animals received care according to institutional animal care committee guidelines. Animal procedures were conducted in compliance with European, national, and institutional guidelines and protocols. For antioxidant treatment, mice were fed on a diet containing 0.7% BHA (Sigma) from 4 weeks of age until sacrifice.

Liver Injury Models

Experiments were performed on male mice between 8 and 10 weeks of age. Murine recombinant TNF (Nenci et al., 2006) or LPS (Sigma) were administered i.p. at concentrations of 10 μg/kg (TNF) or 25 μg/10 g (LPS). Alanine-aminotransferase (ALT) activities, serum cholesterol, triglyceride, glucose, and insulin levels were measured by standard procedures.

Immunoblot Analysis

Protein lysates were prepared from primary hepatocytes or liver samples, separated by SDS-polyacrylamide gel electrophoresis (PAGE), transferred to nitrocellulose, and analyzed by immunoblotting. Membranes were probed with the following antibodies: anti-NEMO (Nenci et al., 2006); anti-Tubulinα (Sigma); anti-phospho-IκBα, anti-JNK, anti-phospho-JNK, anti-cleaved-caspase3, and anti-Bax (Cell Signaling); anti-FADD and anti-caspase-8 (Alexis); anti-cyclinD1 and anti-IκBα (Santa Cruz); anti-IKK2 (Imgenex); and anti-PCNA (Biosource). As secondary antibodies, anti-rabbit-HRP, anti-mouse-HRP, and anti-rat-HRP were used (Amersham). Primary hepatocytes were isolated and cultured as described previously (Luedde et al., 2005).

Quantitative Real-Time PCR

Total RNA was purified from liver tissue using Trizol reagent (Invitrogen). Total RNA (1 μg) was used to synthesize cDNA using SuperScript First-Strand Synthesis System (Invitrogen) and was resuspended in 100 μl of H_2O. cDNA samples (5 μl) were used for real-time PCR, in a total volume of 20 μl using SYBR Green Reagent (Finzyme) and specific primers on a qPCR machine (Opticon 2, MJ Research Inc.). Real-time PCR reactions were performed in triplicates. Primer sequences are available upon request. All values were normalized to the level of ubiquitin mRNA.

Electromobility Shift Assay

Gel retardation assays were performed on nuclear extracts as described previously (Schmidt-Supprian et al., 2000). DNA protein complexes were resolved on a 6% polyacrylamide gel. A 32P-labeled oligonucleotide representing an NF-κB consensus site (5′-CGGGCTG GGGATTCCCCATCTCGGTAC-3′) was used as a probe. For supershifts, antibodies against p50 (sc-114X) and p65 (sc-109X) (Santa Cruz Biotechnology) were used.

TUNEL Assay, BrdU Assay, Immunohistochemistry, and Electron Microscopy

TUNEL test, BrdU assay, immunohistochemistry and electron microscopy were performed by standard procedures. For more detailed information, see the Supplemental Experimental Procedures.

Statistics

Results in Figure S4 are expressed as mean ± SD, whereas error bars in all other figures indicate ±standard error of the mean (SEM). Statistical significance between experimental groups was assessed using an unpaired two-sample Student's t test.

Supplemental Data

The Supplemental Data include Supplemental Experimental Procedures and five supplemental figures and can be found with this article online at http://www.cancercell.org/cgi/content/full/11/2/119/DC1/.

ACKNOWLEDGMENTS

We wish to thank G. Schütz for the Alfp-Cre mice and C. Libbert for recombinant TNF. We thank T. Gillis, T. Tropartz and C. Uthoff-Hachenberg for technical assistance and D. Tosh, M. Lüdde, V. Desmet, C. Netzer and the members of the Pasparakis lab for valuable discussions. This work was supported by EMBL, the University of Cologne and by EU-FP6 grants MUGEN (LSHG-CT-2005-005203) and IMDEMI (MRTN-CT04-005632) to M.P. T.L. was supported by a postdoctoral fellowship from the Schering Foundation Berlin/Germany, Science Office.

Received: August 15, 2006
Revised: November 2, 2006
Accepted: December 5, 2006
Published: February 12, 2007

REFERENCES

Alison, M.R., and Lovell, M.J. (2005). Liver cancer: The role of stem cells. Cell Prolif. *38*, 407–421.

Bandsma, R.H., Wiegman, C.H., Herling, A.W., Burger, H.J., ter Harmsel, A., Meijer, A.J., Romijn, J.A., Reijngoud, D.J., and Kuipers, F. (2001). Acute inhibition of glucose-6-phosphate translocator activity leads to increased de novo lipogenesis and development of hepatic steatosis without affecting VLDL production in rats. Diabetes *50*, 2591–2597.

Beg, A.A., Sha, W.C., Bronson, R.T., Ghosh, S., and Baltimore, D. (1995). Embryonic lethality and liver degeneration in mice lacking the RelA component of NF-κB. Nature *376*, 167–170.

Bentires-Alj, M., Dejardin, E., Viatour, P., Van Lint, C., Froesch, B., Reed, J.C., Merville, M.P., and Bours, V. (2001). Inhibition of the NF-κB transcription factor increases Bax expression in cancer cell lines. Oncogene *20*, 2805–2813.

Brunt, E.M. (2004). Nonalcoholic steatohepatitis. Semin. Liver Dis. *24*, 3–20.

Burke, J.R. (2003). Targeting IκB kinase for the treatment of inflammatory and other disorders. Curr. Opin. Drug Discov. Devel. *6*, 720–728.

Canbay, A., Gieseler, R.K., Gores, G.J., and Gerken, G. (2005). The relationship between apoptosis and non-alcoholic fatty liver disease: An evolutionary cornerstone turned pathogenic. Z. Gastroenterol. *43*, 211–217.

Chaisson, M.L., Brooling, J.T., Ladiges, W., Tsai, S., and Fausto, N. (2002). Hepatocyte-specific inhibition of NF-κB leads to apoptosis after TNF treatment, but not after partial hepatectomy. J. Clin. Invest. *110*, 193–202.

Coffinier, C., Gresh, L., Fiette, L., Tronche, F., Schutz, G., Babinet, C., Pontoglio, M., Yaniv, M., and Barra, J. (2002). Bile system morphogenesis defects and liver dysfunction upon targeted deletion of HNF1β. Development *129*, 1829–1838.

Coleman, R., Genet, S.A., Harper, J.I., and Wilkie, A.O. (1993). Interaction of incontinentia pigmenti and factor VIII mutations in a female with biased X inactivation, resulting in haemophilia. J. Med. Genet. *30*, 497–500.

Courtois, G. (2005). The NF-κB signaling pathway in human genetic diseases. Cell. Mol. Life Sci. *62*, 1682–1691.

Enomoto, N., Takei, Y., Hirose, M., Ikejima, K., Miwa, H., Kitamura, T., and Sato, N. (2002). Thalidomide prevents alcoholic liver injury in rats through suppression of Kupffer cell sensitization and TNF-α production. Gastroenterology *123*, 291–300.

Fang, C.H., Gong, J.Q., and Zhang, W. (2004). Function of oval cells in hepatocellular carcinoma in rats. World J. Gastroenterol. *10*, 2482–2487.

Farrell, G.C., and Larter, C.Z. (2006). Nonalcoholic fatty liver disease: From steatosis to cirrhosis. Hepatology *43*, S99–S112.

Festjens, N., van Gurp, M., van Loo, G., Saelens, X., and Vandenabeele, P. (2004). Bcl-2 family members as sentinels of cellular integrity and role of mitochondrial intermembrane space proteins in apoptotic cell death. Acta Haematol. *111*, 7–27.

Gao, G., and Dou, Q.P. (2000). N-terminal cleavage of bax by calpain generates a potent proapoptotic 18-kDa fragment that promotes bcl-2-independent cytochrome C release and apoptotic cell death. J. Cell. Biochem. *80*, 53–72.

Ghosh, S., and Karin, M. (2002). Missing pieces in the NF-κB puzzle. Cell Suppl. *109* (*Suppl*), S81–S96.

Hanahan, D., and Weinberg, R.A. (2000). The hallmarks of cancer. Cell *100*, 57–70.

Herling, A.W., Burger, H., Schubert, G., Hemmerle, H., Schaefer, H., and Kramer, W. (1999). Alterations of carbohydrate and lipid intermediary metabolism during inhibition of glucose-6-phosphatase in rats. Eur. J. Pharmacol. *386*, 75–82.

International Working Party (1995). Terminology of nodular hepatocellular lesions. Hepatology *22*, 983–993.

Karin, M. (1999). How NF-κB is activated: The role of the IκB kinase (IKK) complex. Oncogene *18*, 6867–6874.

Karin, M., and Lin, A. (2002). NF-κB at the crossroads of life and death. Nat. Immunol. *3*, 221–227.

Kellendonk, C., Opherk, C., Anlag, K., Schutz, G., and Tronche, F. (2000). Hepatocyte-specific expression of Cre recombinase. Genesis *26*, 151–153.

Kojiro, M., and Roskams, T. (2005). Early hepatocellular carcinoma and dysplastic nodules. Semin. Liver Dis. *25*, 133–142.

Lavon, I., Goldberg, I., Amit, S., Landsman, L., Jung, S., Tsuberi, B.Z., Barshack, I., Kopolovic, J., Galun, E., Bujard, H., and Ben Neriah, Y. (2000). High susceptibility to bacterial infection, but no liver dysfunction, in mice compromised for hepatocyte NF-κB activation. Nat. Med. *6*, 573–577.

Lee, J.S., Heo, J., Libbrecht, L., Chu, I.S., Kaposi-Novak, P., Calvisi, D.F., Mikaelyan, A., Roberts, L.R., Demetris, A.J., Sun, Z., et al. (2006). A novel prognostic subtype of human hepatocellular carcinoma derived from hepatic progenitor cells. Nat. Med. *12*, 410–416.

Li, Q., Van Antwerp, D., Mercurio, F., Lee, K.F., and Verma, I.M. (1999a). Severe liver degeneration in mice lacking the IκB kinase 2 gene. Science *284*, 321–325.

Li, Z.W., Chu, W., Hu, Y., Delhase, M., Deerinck, T., Ellisman, M., Johnson, R., and Karin, M. (1999b). The IKKβ subunit of IκB kinase (IKK) is essential for nuclear factor κB activation and prevention of apoptosis. J. Exp. Med. *189*, 1839–1845.

Libbrecht, L., Craninx, M., Nevens, F., Desmet, V., and Roskams, T. (2001). Predictive value of liver cell dysplasia for development of hepatocellular carcinoma in patients with non-cirrhotic and cirrhotic chronic viral hepatitis. Histopathology *39*, 66–73.

Libbrecht, L., Desmet, V., and Roskams, T. (2005). Preneoplastic lesions in human hepatocarcinogenesis. Liver Int. *25*, 16–27.

Luedde, T., Assmus, U., Wustefeld, T., Meyer zu Vilsendorf, A., Roskams, T., Schmidt-Supprian, M., Rajewsky, K., Brenner, D.A., Manns, M.P., Pasparakis, M., and Trautwein, C. (2005). Deletion of IKK2 in hepatocytes does not sensitize these cells to TNF-induced apoptosis but protects from ischemia/reperfusion injury. J. Clin. Invest. *115*, 849–859.

Luedde, T., Liedtke, C., Manns, M.P., and Trautwein, C. (2002). Losing balance: Cytokine signaling and cell death in the context of hepatocyte injury and hepatic failure. Eur. Cytokine Netw. *13*, 377–383.

Maeda, S., Chang, L., Li, Z.W., Luo, J.L., Leffert, H., and Karin, M. (2003). IKKβ is required for prevention of apoptosis mediated by cell-bound but not by circulating TNFα. Immunity *19*, 725–737.

Maeda, S., Kamata, H., Luo, J.L., Leffert, H., and Karin, M. (2005). IKKβ couples hepatocyte death to cytokine-driven compensatory proliferation that promotes chemical hepatocarcinogenesis. Cell *121*, 977–990.

Makris, C., Godfrey, V.L., Krahn-Senftleben, G., Takahashi, T., Roberts, J.L., Schwarz, T., Feng, L., Johnson, R.S., and Karin, M. (2000). Female mice heterozygous for IKKγ/NEMO deficiencies develop a dermatopathy similar to the human X-linked disorder incontinentia pigmenti. Mol. Cell *5*, 969–979.

Marshall, A., Rushbrook, S., Davies, S.E., Morris, L.S., Scott, I.S., Vowler, S.L., Coleman, N., and Alexander, G. (2005). Relation between hepatocyte G1 arrest, impaired hepatic regeneration, and fibrosis in chronic hepatitis C virus infection. Gastroenterology *128*, 33–42.

Motola-Kuba, D., Zamora-Valdes, D., Uribe, M., and Mendez-Sanchez, N. (2006). Hepatocellular carcinoma. An overview. Ann. Hepatol. *5*, 16–24.

Nenci, A., Huth, M., Funteh, A., Schmidt-Supprian, M., Bloch, W., Metzger, D., Chambon, P., Rajewsky, K., Krieg, T., Haase, I., and Pasparakis, M. (2006). Skin lesion development in a mouse model of incontinentia pigmenti is triggered by NEMO deficiency in epidermal keratinocytes and requires TNF signaling. Hum. Mol. Genet. *15*, 531–542.

Oberti, F., Rifflet, H., Flejou, J.F., Leclech, C., Belghiti, J., Rousselet, M.C., and Cales, P. (1997). [Association of hepatic adenomatosis and hepatoportal sclerosis in a woman with incontinentia pigmenti]. Gastroenterol. Clin. Biol. *21*, 147–151.

Okuda, K. (2000). Hepatocellular carcinoma. J. Hepatol. *32*, 225–237.

Pahl, H.L. (1999). Activators and target genes of Rel/NF-κB transcription factors. Oncogene *18*, 6853–6866.

Pasparakis, M., Alexopoulou, L., Episkopou, V., and Kollias, G. (1996). Immune and inflammatory responses in TNFα-deficient mice: A critical requirement for TNFα in the formation of primary B cell follicles, follicular dendritic cell networks and germinal centers, and in the maturation of the humoral immune response. J. Exp. Med. *184*, 1397–1411.

Pasparakis, M., Courtois, G., Hafner, M., Schmidt-Supprian, M., Nenci, A., Toksoy, A., Krampert, M., Goebeler, M., Gillitzer, R., Israel, A., Krieg, T., Rajewsky, K., and Haase, I. (2002). TNF-mediated inflammatory skin disease in mice with epidermis-specific deletion of IKK2. Nature *417*, 861–866.

Pfeffer, K., Matsuyama, T., Kundig, T.M., Wakeham, A., Kishihara, K., Shahinian, A., Wiegmann, K., Ohashi, P.S., Kronke, M., and Mak, T.W. (1993). Mice deficient for the 55 kd tumor necrosis factor receptor are resistant to endotoxic shock, yet succumb to L. monocytogenes infection. Cell *73*, 457–467.

Pikarsky, E., Porat, R.M., Stein, I., Abramovitch, R., Amit, S., Kasem, S., Gutkovich-Pyest, E., Urieli-Shoval, S., Galun, E., and Ben Neriah, Y. (2004). NF-κB functions as a tumour promoter in inflammation-associated cancer. Nature *431*, 461–466.

Ramadori, G., and Armbrust, T. (2001). Cytokines in the liver. Eur. J. Gastroenterol. Hepatol. *13*, 777–784.

Rudolph, D., Yeh, W.C., Wakeham, A., Rudolph, B., Nallainathan, D., Potter, J., Elia, A.J., and Mak, T.W. (2000). Severe liver degeneration and lack of NF-κB activation in NEMO/IKKγ-deficient mice. Genes Dev. *14*, 854–862.

Schmidt-Supprian, M., Bloch, W., Courtois, G., Addicks, K., Israel, A., Rajewsky, K., and Pasparakis, M. (2000). NEMO/IKKγ-deficient mice model incontinentia pigmenti. Mol. Cell *5*, 981–992.

Schwabe, R.F., and Brenner, D.A. (2006). Mechanisms of liver injury. I. TNF-α-induced liver injury: Role of IKK, JNK, and ROS pathways. Am. J. Physiol. Gastrointest. Liver Physiol. *290*, G583–G589.

Sherman, M. (2005). Hepatocellular carcinoma: Epidemiology, risk factors, and screening. Semin. Liver Dis. *25*, 143–154.

Strasser, A., and Newton, K. (1999). FADD/MORT1, a signal transducer that can promote cell death or cell growth. Int. J. Biochem. Cell Biol. *31*, 533–537.

Tamura, H., Ohtsuru, A., Kamohara, Y., Fujioka, H., Yanaga, K., Kanematsu, T., and Yamashita, S. (2003). Bax cleavage implicates caspase-dependent H2O2-induced apoptosis of hepatocytes. Int. J. Mol. Med. *11*, 369–374.

Tanaka, M., Fuentes, M.E., Yamaguchi, K., Durnin, M.H., Dalrymple, S.A., Hardy, K.L., and Goeddel, D.V. (1999). Embryonic lethality, liver degeneration, and impaired NF-κB activation in IKK-β-deficient mice. Immunity *10*, 421–429.